Journal of Solid State Electrochemistry
https://doi.org/10.1007/s10008-023-05452-7

ORIGINAL PAPER

Convex optimization for maximizing the degradation efficiency of chloroquine in a flow-by electrochemical reactor

Alejandro Regalado-Méndez[1] · Juliana Zavaleta-Avendaño[1] · Ever Peralta-Reyes[1] · Reyna Natividad[2]

Received: 13 December 2022 / Revised: 9 February 2023 / Accepted: 3 March 2023
© The Author(s), under exclusive licence to Springer-Verlag GmbH Germany, part of Springer Nature 2023

Abstract

The degradation efficiency of chloroquine phosphate (CQ), an anti-COVID-19 drug, was investigated in a flow-by electrochemical reactor (FBER) provided with two boron-doped diamond (BDD) electrodes (as cathode and anode) under batch recirculation mode. A central composite rotatable design (CCRD) was run down to model and assess the influence of initial pH in an interval of 3.71 to 11.28, the current density in an interval of 34.32 to 185.68 mA cm^{-2}, and liquid volumetric flow rate in an interval of 0.58 to 1.42 L min^{-1}, and conduct the convex optimization to obtain the maximum degradation efficiency. Experimental results were modeled through a second-order polynomial equation having a determination coefficient (R^2) of 0.9705 with a variance coefficient of 1.1%. Optimal operating conditions found (initial pH of 5.38, current density (j) of 34.4 mA cm^{-2}, and liquid flow rate (Q) of 1.42 L min^{-1}) led to a global maximum degradation efficiency, COD removal efficiency, and mineralization efficiency of 89.3, 51.6 and 53.1%, respectively, with an energy consumption of 0.041 kWh L^{-1} within 9 h of treatment. Additionally, a pseudo-zero-order kinetic model was demonstrated to fit the experimental data and the calculated pseudo-zero-order kinetic constant (k_{app}) was 13.14 mg L^{-1} h^{-1} (2.54×10^{-5} mol dm^{-3} h^{-1}). Furthermore, the total operating cost was of 0.47 US$ L^{-1}. Finally, this research could be helpful for the treatment of wastewater containing an anti-COVID-19 drug such as CQ.

Keywords Chloroquine · Convex optimization · Anti-COVID-19 drug · Degradation · Flow-by electrochemical reactor

Nomenclature

Symbols meaning

A	Matrix that contains quadratic coefficients terms of the quadratic equation
A_e	Electrode area (cm^2)
B	Vector that contains the linear coefficient terms of the quadratic equation
C	Constant term of the quadratic equation
Cost	Total operational cost (US$/L)
COD	Chemical oxygen demand (mg L^{-1})
E_C	Energy consumption (kWh L^{-1})
H	Hessian matrix
j	Current density (mA cm^{-2})
k_{app}	Apparent kinetic constant (mg L^{-1} h^{-1})
pH	Logarithmic scale of acidity or basicity (dimensionless)
Q	Liquid flowrate (L min^{-1})
q	Quantity of chemical utilized (g)
R^2	Determination coefficient
t	Reaction time (h)
TOC	Total organic carbon (mg L^{-1})
U	Mean cell voltage (V)
X	Uncoded independent variables
x	Coded independent variables
V_s	Synthetic solution volume (L)
[·]	Concentration (mg L^{-1})

Acronyms

ANOVA	Analysis of variance
BDD	Boron-doped diamond
CCRD	Central composite rotatable design
CQ	Chloroquine phosphate
EDCQ	Electrochemical degradation of chloroquine phosphate
FBER	Flow-by electrochemical reactor

✉ Alejandro Regalado-Méndez
alejandro.regalado33@gmail.com; regalado@angel.umar.mx

[1] Investigation Laboratories, Universidad del Mar, Puerto Ángel, 70902 Oaxaca, México

[2] Chemical Engineering Laboratory, Centro Conjunto de Investigación en Química Sustentable, UAEMex-UNAM, Universidad Autónoma del Estado de México, Estado de México, Toluca 50200, México

Published online: 11 April 2023

F-value	Value of the *F* distribution
MOC	Mean oxidation number of carbon
p-value	Measure of the probability that an observed difference
RMSE	Root-mean-square error

Greek letters

α	Rotatability factor ($\alpha = 2^{k/4}$)
β	Coefficients of the adjusted quadratic model
ξ	Electrical energy price (0.071 US$ (kWh)$^{-1}$)
Ω:	Stirring speed (rpm)
λ	Eigenvalues
ϕ	Electrolyte price (0.033 US$ g^{-1})
η	Degradation efficiency (%)

Subscripts

Adj	Adjusted
Exp	Experimental
i	Variable number
k	Variable number different to *i*
n	Number of experiments
Pred	Predicted
0	Initial

Introduction

Since the beginning of the year 2020, the whole world has faced a great health challenge unprecedented in humanity because the outbreak of the COVID-19 pandemic due to the new coronavirus (SARS-CoV-2). The total worldwide number of infections as of 07 December 2022 is over 641 million confirmed cases and more than 6.6 million deaths [1]. In Mexico, as of 7 December 2022 are over 7.1 million confirmed infections and more than 331 thousand deaths [2]. To mitigate COVID-19 infections and reduce the mortality rate, several epidemiological researchers and virologists from various world regions have developed and tested alternative anti-COVID-19 treatments. Among the most widely applied treatments against the coronavirus because of their effectiveness are those that use the drugs ribavirin [3], chlorpromazine [4], favipiravir [5], remdesivir [6], chloroquine [7], and hydroxychloroquine [8]. Even when the World Health Organization (WHS) has not recommended any of these drugs as treatment for COVID-19, health organizations and hospitals in several countries, including the USA and Mexico, have used chloroquine (CQ) and hydroxychloroquine (HCQ) as an alternative anti-COVID-19 treatment to mitigate the death rate because of their effectiveness against malaria virus and anti-inflammatory properties [9]. However, these drugs fall in the category of persistent contaminants of water because of their low biodegradability. CQ is an anti-inflammatory drug like ibuprofen but with a broader spectrum [10]. The chemical structure of CQ is depicted in Table 1, and it belongs to the group of aminoquinolines [11]. It is a white, odorless, and crystalline powder with a bitter taste, which is soluble in water and highly soluble in chloroform and ether [12]. This drug is highly toxic and can cause seizures, coma, and heart failure [11] at doses greater than 220 mg kg^{-1} [13]. Due to CQ poorly biodegradability, it cannot be treated in conventional wastewater

Table 1 Synthetic wastewater quality and physical properties of CQ

Molecule of chloroquine	Synthetic wastewater quality				
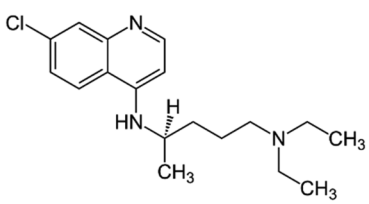	**[*CQ*] (mg L^{-1})**	**pH**	**Conductivity (µS cm^{-1})**	***TOC* (mg L^{-1})**	***COD* (mg L^{-1})**
Condensed formula: $C_{18}H_{26}ClN_3 \cdot 2H_3PO_4$ **CAS No.: 50–63-5**	150	5.2*	14,690*	62.81*	82.67*
	Physicochemical properties				
	Property				**value**
	Molar weight (g mol^{-1})				515.86 [37]
	Melting point (°C)				192–197 [37]
	Boiling temperature (°C)				460 [38]
	p_{ka} at 25 °C				10.32 [39]
	Log (K_{ow})				4.66 [38]
	Solubility in water (g L^{-1}) at 25 °C				50.0 [37]
	Henry's law constant (atm m^{-3} mol^{-1})				1.1×10^{-12} [39]
	λ_{max} (nm)				220 [40]

*Mean value of the total number of experiments

treatment plants (e.g., activated sludge), in this sense, the advanced oxidation processes (e.g., electro-oxidation, photodegradation, among others) are most appropriate to remove this type of pollutants because of their effectiveness since a 90% of degradation is achieved [14]. There are few studies on assisted degradation of CQ in an aqueous environment, which mainly focus on photochemical stability [15], alkaline hydrolysis and chemical oxidation with H_2O_2 [16], electro-Fenton [17], and photodegradation [18]. Electrochemical degradation is a green technology that has been rising interest in the last years because of its low energy consumption and high effectiveness in the degradation of persistent pollutants such as 4-chlorophenol [19], 2-chlorophenol [20], and ibuprofen [21], among others [22, 23]. Although there are few degradation studies (photodegradation and electro-Fenton) of CQ, which employ anodes of graphite, Pt, and BDD to produce hydrogen peroxide (H_2O_2) as an oxidant agent, the optimization of the degradation of CQ has not been reported. Also, the electro-oxidation has not been yet employed to perform the degradation of CQ. In this context, BDD anodes have negligible interaction with the hydroxyl radical ($^{\bullet}OH$) generated on their surface [24] implying high oxidation efficiency [25]. Additionally, electro-oxidation does not require any additional reagents because only uses electrical energy as a unique reagent [21], where the electron flow is the green reagent [26] that drives the electrolysis process to produce $^{\bullet}OH$.

Concerning the optimization of the electrochemical processes, many works employ the response surface methodology (RSM) as a popular method. RSM is mainly driven by experimental designs, which include central composite rotatable (CCR) [27], Box-Behnken [28], Taguchi [29], Plackett–Burman [30], and others [31, 32]. CCR design is the most used because provides sufficient data for testing a lack of fit. In the electrochemical degradation of emerging pollutants through optimization DoE-driven, the studied standard variables include the initial potential of hydrogen (pH_0), current intensity (I), or current density (j), initial concentration ($[C]_0$), for batch reactors the stirring speed (Ω), and for flow-by reactors, the volumetric flow rate (Q), while the common responses are electrochemical degradation efficiency (η) [33], color removal efficiency (%CR) [34], *COD* removal efficiency (%COD) [35], *TOC* removal efficiency (%TOC) [36], and energy consumption (E_C) [21]. Although the literature on parametric optimization by RSM is abundant, convex optimization has not been widely addressed in the electrochemical degradation processes even though it is widely implemented by students and researchers from industry and academia.

In this work, the maximizing electrochemical degradation of chloroquine phosphate (EDCQ) was carried out in a FBER in batch recirculation mode by the convex optimization method. The FBER is equipped with two BDD electrodes. To complete the optimization objective a CCRD was used to model and evaluate the effect on the degradation efficiency of many operating variables, namely initial pH, current density (j), and liquid volumetric flow rate (Q). Also, the total operating cost, model validation, and kinetic modeling were computed. This research is justified in the context of the intensive use assumption of CQ as an anti-COVID-19 drug and significant production of pharmaceutical wastewater.

Materials and methods

Reagents and aqueous chloroquine phosphate solution

All reagents were commercially available and used as received. The chloroquine phosphate (CQ), sodium hydroxide (NaOH), and sulfuric acid (H_2SO_4) were purchased from Sigma-Aldrich Company, with a purity of 98.5%, 97%, and 95%, respectively. Meanwhile, the sodium sulfate (Na_2SO_4) was purchased from Karal Group with a purity of 99%.

Synthetic wastewater of CQ (150 mg L^{-1} or 62.81 mg of TOC L^{-1}) with 0.1 M of Na_2SO_4 as a supporting electrolyte was freshly prepared each day for each experiment. This synthetic solution was then added into the reservoir of the experimental set-up to homogenize it by recirculating it for 10 min through the experimental set-up without applying any current density. Additionally, distillate water was used for preparing all synthetic wastewater solutions of CQ. Table 1 displays the chemical structure and physicochemical properties of CQ.

Experimental system

The experimental system was made-up of a flow-by electrochemical reactor (active area of 32 cm^2, interelectrode gap of 1.1 cm, and effective volume of 35.2 cm^3) provided with two BDD electrodes, a polycarbonate vessel tank (volume of 3.5 L), a magnetic pump of 300 rpm, a glass rotameter, a tubing of 0.635 cm radius, and valves and connectors of Master-Flex^{MT} quality. A full description can be found in an authors' previous work [41]. A representative chart diagram of the experimental system is depicted in Fig. 1.

Electrochemical degradation of CQ

A total of 2.5 L of aqueous CQ solution (V_s) were added into the reservoir of the experimental system (see Fig. 1). The analyzed operational variables were initial pH (pH_0), current density (j), and liquid flowrate (Q), according to Table 2. The lower, center, higher, and axial levels of each operational factor that appeared in Table 2 are coded as $-\alpha$, -1, 0, $+1$, and $+\alpha$, respectively.

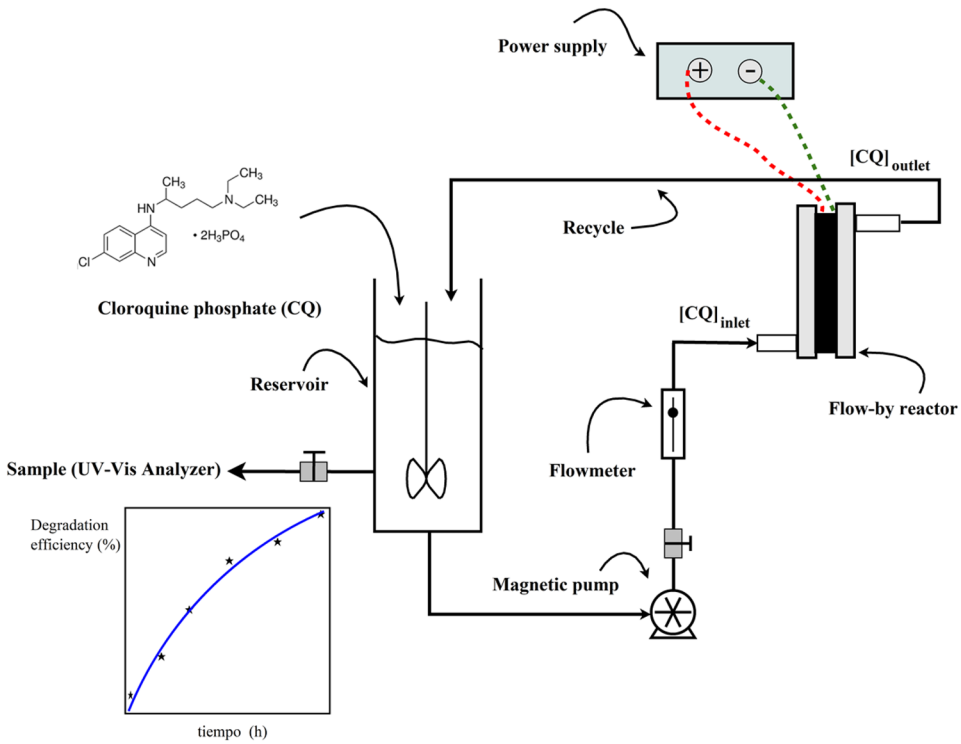

Fig. 1 Experimental system for the EDCQ in a flow-by reactor under batch recirculation mode

The design space and the 17 runs for the optimization of the electrochemical degradation process of CQ are presented in Table 3. The experimental design was a central composite rotatable one (CCRD, 8 factorial points, 6 axial points, and 3 center points, where $\alpha = \pm 1.68$, giving 17 runs).

In an electrochemical process, the potential of hydrogen (pH) is one of the most important variables since the process is conducted in an aqueous solution. Therefore, pH must be chosen according to the hydrophilic and lipophilic properties of the contaminant to be degraded; in this case, the pH must be lower than 11.5 since the solubility decreases at higher values than 11.5, the current density (j) was specified by a typical range used in the electro-oxidation processes [22], the range of volumetric flow rate (Q) was selected according to previous authors works, where other organic molecules (e.g., ibuprofen and 2-chlorophenol) have been degraded with the same reactor [20, 21]. The operational factors analyzed on this research can be encrypted by applying Eq. (1),

$$x_i = \frac{X_i - X_{i,0}}{\Delta X_i} \tag{1}$$

Table 2 Numeric values and levels of the operating factor

Operating parameters	Levels				
	-α	-1	0	+1	+α
X_1: pH_0	3.72	5.25	7.5	9.75	11.28
X_2: j (mA cm^{-2})	34.32	65.00	110.0	155.00	185.68
X_3: Q (L min^{-1})	0.58	0.75	1.0	1.25	1.42

Chemical analysis

The absorption spectra for each run of the CCRD were obtained and recorded after 9 h of treatment using a Lamda 365 PerkinElmer UV–visible spectrophotometer, UV–visible spectra of the synthetic solution of CQ at 150 mg L^{-1} in 0.1 M Na_2SO_4 were initially recorded. The absorption spectra of the same solution were then recorded at different times when the FBER operate under optimal operating conditions. Also, all UV–visible spectra of samples were acquired between 200 and 400 nm, identifying 220 nm as the wavelength of maximum absorption of CQ. COD was determined according to standard methods for the analysis of wastewater [42], and the total organic carbon (TOC) was measured by a 6001 TOC analyzer Shimadzu for the optimal operating point of the electrochemical degradation of CQ. The pH of all synthetic wastewater solutions of CQ was measured by using a HI2210 Hanna potentiometer.

Analytical procedures

The degradation efficiency was computed by using Eq. (2). Energy consumption per L was estimated by using Eq. (3). The total operational cost (cost) of the CQ degradation includes energy consumption (E_C (kWh L^{-1})) and electrolyte cost ($C_{electrolyte}$ (g L^{-1})), which can be calculated by the set of Eqs. (3), (4), and (5). The percentage of mineralization efficiency was computed according to Eq. (6),

$$\eta(\%) = \frac{[CQ]_0 - [CQ]_t}{[CQ]_0} \times 100 \tag{2}$$

$$E_C = \frac{U \times j \times A_e \times t}{V_s} \tag{3}$$

$$C_{electrolyte} = \frac{q_{Na_2SO_4}}{V_s} \tag{4}$$

$$\text{Cos}t = \xi E_C + \phi C_{electrolyte} \tag{5}$$

$$ME(\%) = \frac{TOC_0 - TOC_t}{TOC_0} \times 100 \tag{6}$$

where U is the mean cell voltage (V), V_s is the synthetic solution volume (L), A_e is the electrode area (cm^2), j is the current density (mA cm^{-2}), t is the degradation time (h), ξ is the electricity cost (0.071 US\$ $(kWh)^{-1}$) provided by a Mexican Electricity company in December 2022, taking into consideration that 1 US\$ $(20\ MXP)^{-1}$), ϕ is the price of electrolyte (0.033 US\$ g^{-1}), and q is the quantity of used chemicals (g).

Optimization process

To accomplish the optimization process, the first step was to propose a model of the observed response (η) in the function of the selected operational variables (e.g., initial pH, current density, and liquid flow rate) employing a second-order polynomial model like Eq, (7),

$$\eta = \beta_0 + \sum_{i=1}^{k} \beta_i x_i + \sum_{i=1}^{k} \beta_{ii} x_i^2 + \sum_{i=1}^{k-1} \sum_{k=i+1}^{k} \beta_{i,k} x_i x_k + \varepsilon \tag{7}$$

where η is the modeled response, β values are the coefficients of the polynomial, ε is the random error, and x_i and x_j are the encrypted independent variables. The β values were computed by applying the stepwise regression method. To evaluate the suitability of the model fitted and the importance of the terms of the second-order polynomial an analysis of variance (ANOVA) was performed. Reduced root-mean-square error (RMSE) is often used to demonstrate the fitted model accuracy of responses (e.g., η, have a look at Eq. (8)),

$$RMSE = \sqrt{\frac{1}{n} \sum_{n} \left(\frac{\eta_{n,\,\mathrm{Pr}ed} - \eta_{n,\,Exp}}{\eta_{n,\,Exp}} \right)^2} \tag{8}$$

where $\eta_{n,\,\mathrm{Pred}}$ is the modeled response, $\eta_{n,\,\mathrm{Exp}}$ is the experimental response, and n is the total amount of runs.

The second step was to write the quadratic polynomial model in matrix form equal to Eq. (9); therefore, this equation must be a concave function.

$$\eta = x^T A x + Bx + C \tag{9}$$

where $x = [x_1, x_2, \ldots, x_n]^T$, A, is the matrix that contains the coefficients terms of the quadratic equation; B is the vector that contains the linear coefficient terms of the quadratic equation, and C is the constant term of the quadratic equation.

The third step was to prove that Eq. (9) was a concave function by means of convex optimization. Hence, the eigenvalues (λ_1, λ_2, and λ_3) of the Hessian matrix (H, Eq. (10)) must be equal to or less than zero.

$$H = \frac{\partial}{\partial x^T \partial x} \left(x^T A x + Bx + C \right) = 2A \tag{10}$$

The fourth step was to rewrite the original optimization problem (maximization of η) in an optimization standard problem form like Eq. (11). The fifth step and last one was to solve numerically the minimization problem. To find the optimal point, the MATLAB. R2017a ® software package was employed. Also, three different algorithms (such as "active-set," "sqp," and "interior-point") were used. Moreover, a general pseudo-code to solve the optimization problem given by Eq. (11) is presented in the supported material (see Table S1).

$$\begin{aligned} &Min \quad \eta = x^T A x + Bx + C \\ &s.t. \\ &\quad x_1^2 \le \alpha^2 \\ &\quad x_2^2 \le \alpha^2 \\ &\quad x_3^2 \le \alpha^2 \\ &\alpha: \ \ rotatability\ (1.68) \end{aligned} \tag{11}$$

Results and discussion

Model fitting

In this research, the Design Expert® V.10.0 software was employed to conduct the CCRD, regression analysis, and model fitting. The seventeen runs of the CCRD are shown in Table 3. In this case of study, runs 2, 3, 9, 10, 13, and 17 are axial points; runs 1, 4, 5, 7, 8, 11, 14, and 16 are factorial points; and runs 15, 12, and 6 are center points. The reported (See Table 3) experimental values of the degradation efficiency (η) of CQ are in the interval of 74.9–86.3%. Given the experimental response (η) in the function of the mathematical relationship between independent process factors, a second-order polynomial has been fitted (see Eq. (12)).

Table 3 CCRD of initial pH (X_1), current density (X_2), liquid flowrate (X_3), and their observed response (degradation efficiency (η), %) using a FBER

Std	Run	Design space	Actual variables			Coded variables			Response
			X_1	X_2 (mA cm^{-2})	X_3 (L min^{-1})	x_1	x_2	x_3	η (%)
6	1	Factorial	9.75	65.00	1.25	1.00	−1.00	1.00	84.0
13	2	Axial	7.50	110.00	0.58	0.00	0.00	−1.68	81.3
11	3	Axial	7.50	34.32	1.00	0.00	−1.68	0.00	86.3
1	4	Factorial	5.25	65.00	0.75	−1.00	−1.00	−1.00	82.3
8	5	Factorial	9.75	155.00	1.25	1.00	1.00	1.00	76.5
16	6	Center	7.50	110.00	1.00	0.00	0.00	0.00	79.8
4	7	Factorial	9.75	155.00	0.75	1.00	1.00	−1.00	76.9
2	8	Factorial	9.75	65.00	0.75	1.00	−1.00	−1.00	83.5
10	9	Axial	11.28	110.00	1.00	1.68	0.00	0.00	77.8
9	10	Axial	3.72	110.00	1.00	−1.68	0.00	0.00	76.8
7	11	Factorial	5.25	155.00	1.25	−1.00	1.00	1.00	77.8
17	12	Center	7.50	110.00	1.00	0.00	0.00	0.00	78.3
14	13	Axial	7.50	110.00	1.42	0.00	0.00	1.68	80.8
5	14	Factorial	5.25	65.00	1.25	−1.00	−1.00	1.00	84.7
15	15	Center	7.50	110.00	1.00	0.00	0.00	0.00	78.2
3	16	Factorial	5.25	155.00	0.75	−1.00	1.00	−1.00	74.9
12	17	Axial	7.50	185.681	1.00	0.00	1.68	0.00	76.4

Equation with coded factors,

$$\eta = 78.76 + 0.21x_1 - 3.29x_2 + 0.33x_3 + 0.025x_1x_2 - 0.65x_1x_3 - 0.05x_2x_3 - 0.49x_1^2 + 0.94x_2^2 + 0.83x_3^2 \quad (12)$$

Equation with uncoded factors,

$$\eta = 89.22 + 2.69X_1 - 0.17X_2 - 16.09X_3 + 0.0002X_1X_2 - 1.16X_1X_3 - 0.004X_2X_3 - 0.09X_1^2 + 0.0005X_2^2 + 13.29X_3^2$$

Analysis of variance (ANOVA)

Table 4 shows the ANOVA results for the obtained second-order polynomial regression model. The ANOVA analysis indicates that the fitted model is statistically suitable for the representation of the electrochemical degradation of CQ at the studied process variables range (in a FBER equipped with two BDD electrodes). A model F-value of 25.56 indicates that the fitted model is significant with only a 0.01% probability that the F-value of a model this large could be

Table 4 ANOVA for the quadratic polynomial

Source	Sum of squares	Degree of freedom	Mean Square	*F-value*	*p-value*	Remark
Degradation efficiency η (%)						
Model	178.3374	9	19.8153	25.5570	0.0001	*Significant*
x_1	0.6081	1	0.6081	0.7843	0.4052	
x_2	148.6052	1	148.6052	191.6656	< 0.0001	
x_3	1.5219	1	1.5219	1.9629	0.2039	
x_1x_2	0.0050	1	0.0050	0.0069	0.9382	
x_1x_3	3.3800	1	3.3800	4.3594	0.0752	
x_2x_3	0.0200	1	0.0200	0.0258	0.8769	
x_3^2	2.7618	1	2.7618	3.5620	0.1011	
x_1^2	9.8963	1	9.8963	12.7639	0.0091	
x_2^2	7.7825	1	7.7825	10.0376	0.0157	
Residual	5.4274	7	0.7753			
Lack of fit	3.8207	5	0.7641	0.9512	0.5842	*Not significant*
Pure error	1.6067	2	0.8033			
Cor total	183.7647	16				

x_3^2; adequate precision = 16.871; *C.V.* (%) = 1.10

due to noise since the p-value (0.0001) is less than 0.05 [43]. In this study, x_2, x_1x_3, x_1^2, x_2^2, and x_3^2 (p-values: 0.0001, 0.0752, 0.1011, 0.0091, and 0.0157) are significant model terms of the second-order polynomial since the p-value is very close to or less than 0.1. A lack of fit F-value of 0.5842 indicates that the lack of fit is not significant, which is reasonable since it was specified to fit the experimental response (η_{Exp}) to a second-order polynomial. A determination coefficient (R^2) value of 0.9705 for η indicates a very good model fitting [44]. Moreover, the RMSE for response (η) gives a value of 0.007 indicating that the model regression fitted (Eq. (12)) for the degradation efficiency (η) is in concordance with the experimental results. Also, the $R^2_{\mathrm{Pr}ed}$ of 0.8202 is reasonable with the R^2_{Adj} of 0.9325 since the difference between both ($R^2_{Adj} - R^2_{Pred}$) is less than 0.2. An adequate precision ratio of 16.871 means an adequate signal because this value is greater than 4 [45]. Hence, the second-order polynomial fitted here can be employed to model the response in the design space (CCRD). Furthermore, the given small value of the coefficient of variance (C.V. of 1.1% for η) revealed great accuracy of the performed tests since the C.V. was under 10%, which indicates that the model fitted has high reproducibility [46].

The parity plot (see Fig. 2a) and the normal percentage probability residual versus studentized residual (see Fig. 2b) demonstrate the model adequacy to predict the response (η). Figure 2a reveals a high-quality correlation between experimental response(η_{Exp}) and predicted response (η_{Pred}). Figure 2b shows a normal distribution because the scattering points fall within a 45-straight line. Therefore, the experimental data has a normal distribution. Furthermore, the outlier-t values lie in the range of ± 1.02, suggesting that the model fitting the response was reasonably good with practically no data register error because there is a high reproducibility. Also, no data transformation is necessary.

Interaction effects amongst operating factors

Analyzing Eq. (12) in terms of coded parameters, a negative β value in the second-order model indicates an adverse effect among operating parameters; meanwhile, a positive β value indicates a beneficial effect on its operational parameters. Analyzing the β values of Eq. (12) in coded terms, the degradation efficiency (η) had a favorable effect with x_1 (j) and x_3 (Q) but decreases with x_1 (pH_0). Similarly, the degradation efficiency increases with the interaction term between initial pH and current density x_1x_2 ($pH_0 \times j$) but had an unfavorable effect with interaction terms between initial pH and liquid flow rate x_1x_3 ($pH_0 \times Q$) and between current density and liquid volumetric flow rate x_2x_3 ($j \times Q$).

To evaluate the effect of each coefficient (β values) on the quadratic model multiple regression, a Pareto analysis was performed by using Eq. (13),

$$\eta = x^T \begin{bmatrix} -0.49 & 0.0125 & -0.325 \\ 0.0125 & 0.94 & -0.025 \\ -0.325 & -0.025 & 0.83 \end{bmatrix} x + \begin{bmatrix} 0.21 \\ -3.29 \\ 0.33 \end{bmatrix} x + 78.76 \tag{13}$$

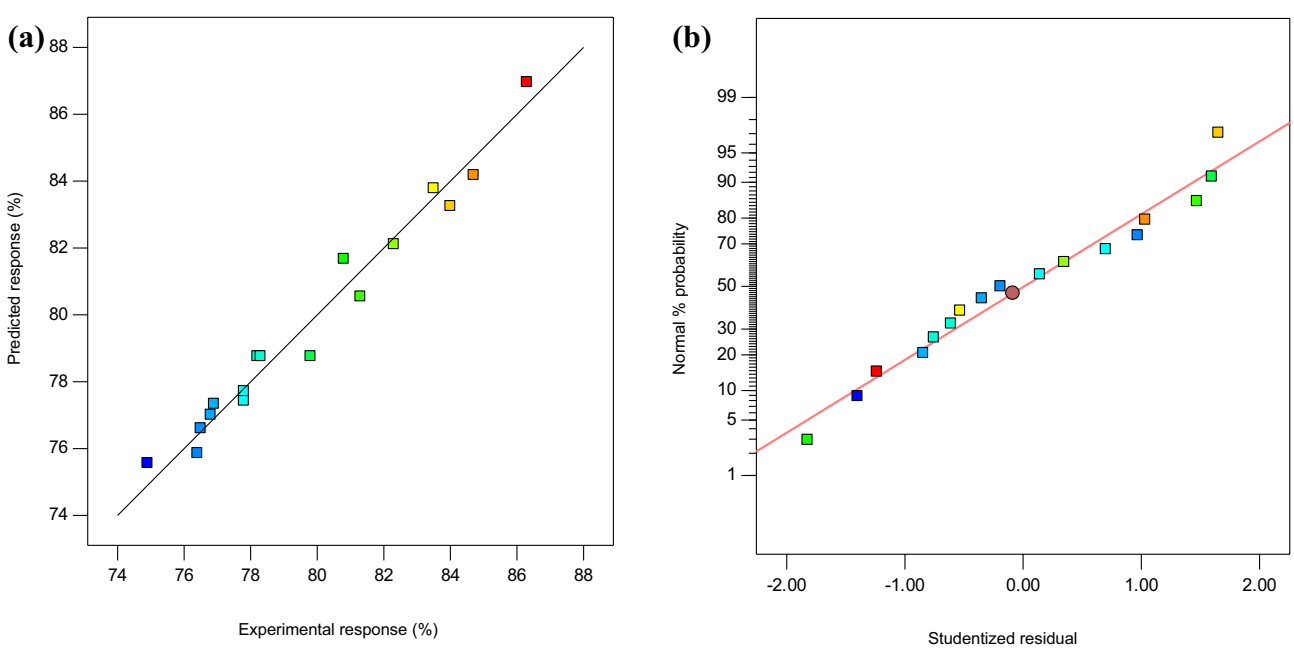

Fig. 2 **(a)** Experimental response versus predicted response for η; **(b)** normal percentage probability residual versus studentized residual for η

Figure 3 displays the Pareto graphic analysis. The results in this figure indicate that among the variables, β_0 (constant term, %) produces the largest effect (92.05%) on the response (η). Also, the term β_2 (current density, mA cm^{-2}), produces a medium effect (3.84%) on the response (η). These results suggest that the most important variable is the current density (j), and this agrees with the fact that at high current density, the hydroxyl radicals are increased.

Figure 4 depicts the 2-D contour plots of the degradation efficiency of CQ by means of electro-oxidation. In the electrochemical degradation of organic compounds (e.g., chloroquine), the pH plays an important role because it controls the hydroxyl radical. Therefore, from Fig. 4a a high electro-degradation is attained closely to 8.0 and from Fig. 4b a high electro-degradation is attained closely to 11.2. Hence, no obvious difference in degradation efficiency can be found when pH was in the range of 2.8–11.2. From Fig. 4a and b, a high electro-degradation is attained closely to 1.0 L min^{-1}, which is consistent with the reported in other studies from electrochemical degradation of organic compounds (e.g., ibuprofen and 2-chlorophenol) using the same FBER [20, 21]. Also, from Fig. 4c, it can be seen that the degradation efficiency decreases when increases the current density (from 20 to 200 mA cm^{-2}). This could be ascribed to the abatement of hydroxyl radicals production on the surface of the BDD electrode since other oxidant agents (e.g., O_2, O_3, and H_2O_2, 2.42 V, 2.07 V, and 1.78 V, respectively) have been produced simultaneously [47], which have lesser oxidation potential than the oxidation potential (2.8 V) of hydroxyl radicals. Additionally, Fig. 4b shows that at medium values of volumetric flow rate increase because the contaminant is relatively easy diffuse on the BDD electrode surface were there are high amount of hydroxyl radicals ready to react with the contaminant. Figure 4c shows that the degradation efficiency decreases at relatively high volumetric flow rate because the contaminant has not had enough contact time to react with the $^{\bullet}$OH formed on the BDD electrode surface. Moreover, even though a significant effect of pH on degradation efficiency was expected, in this study a moderate effect is shown. This is given by a decreased-on hydroxyl radical production on the BDD electrode surface. Hence, the hydroxyl anion (OH^-) is favorable. Finally, hydroxyl radicals are expected to be produced on the BDD anode surface at acid and neutral pH and by direct oxidation of hydroxyl anion at a pH ≥ 10. This mechanism is expected to be very slow though [48].

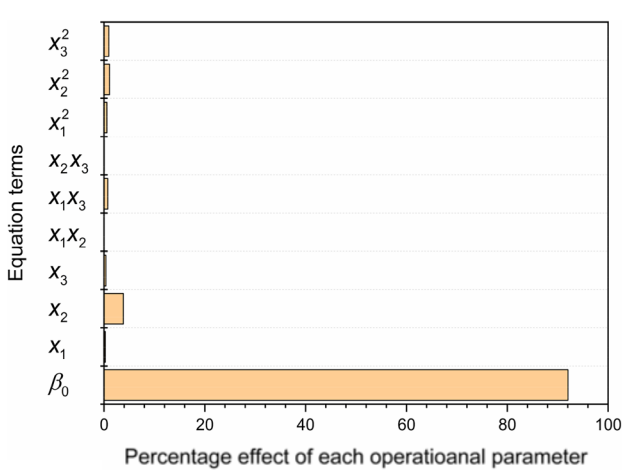

Fig. 3 Pareto chart analysis

Convex optimization of electrochemical degradation of chloroquine

The quadratic polynomial (Eq. (12) can be written in matrix form (see Eq. (14)) to determine the Hessian matrix according to Eq. (10). At this point, the eigenvalues of the Hessian matrix (see Eq. (15) are used to verify if the objective function (η) is concave. The eigenvalues of the Hessian matrix were $\lambda_1 = -1.13$, $\lambda_2 = 1.78$, and $\lambda_3 = 1.91$, which indicate that the concavity of the surface (see Eq. (14)) is inconsistent [49]. Also, Eq. (14) has a negative curvature, indicating that there is a critical point [50], which is called a saddle point because their surface form is given by hyperboles. Moreover, the saddle point is a serious candidate to be an optimal point.

$$\eta = x^T \begin{bmatrix} -0.49 & 0.0125 & -0.325 \\ 0.0125 & 0.94 & -0.025 \\ -0.325 & -0.025 & 0.83 \end{bmatrix} x + \begin{bmatrix} 0.21 \\ -3.29 \\ 0.33 \end{bmatrix} x + 78.76 \tag{14}$$

$$H = \begin{bmatrix} -0.980 & 0.025 & -0.650 \\ 0.025 & 1.880 & -0.050 \\ -0.650 & -0.050 & 1.660 \end{bmatrix} \tag{15}$$

The convex optimalization problem to be solved is expressed by Eq. (16). The optimal operating point found is listed in Table 5. This table indicates that a local maximum was achieved when the convex optimalization problem was solved numerically by using different methods. All methods used find a unique optimal operating point. For this convex optimization problem, the *Active-set* method solves it in only seven iterations.

$$\begin{aligned} &Min \quad \eta = x^T \begin{bmatrix} -0.49 & 0.0125 & -0.325 \\ 0.0125 & 0.94 & -0.025 \\ -0.325 & -0.025 & 0.83 \end{bmatrix} x + \begin{bmatrix} 0.21 \\ -3.29 \\ 0.33 \end{bmatrix} x + 78.76 \\ &s.t. \\ &\quad x_1^2 \le (1.68)^2 \\ &\quad x_2^2 \le (1.68)^2 \\ &\quad x_3^2 \le (1.68)^2 \end{aligned} \tag{16}$$

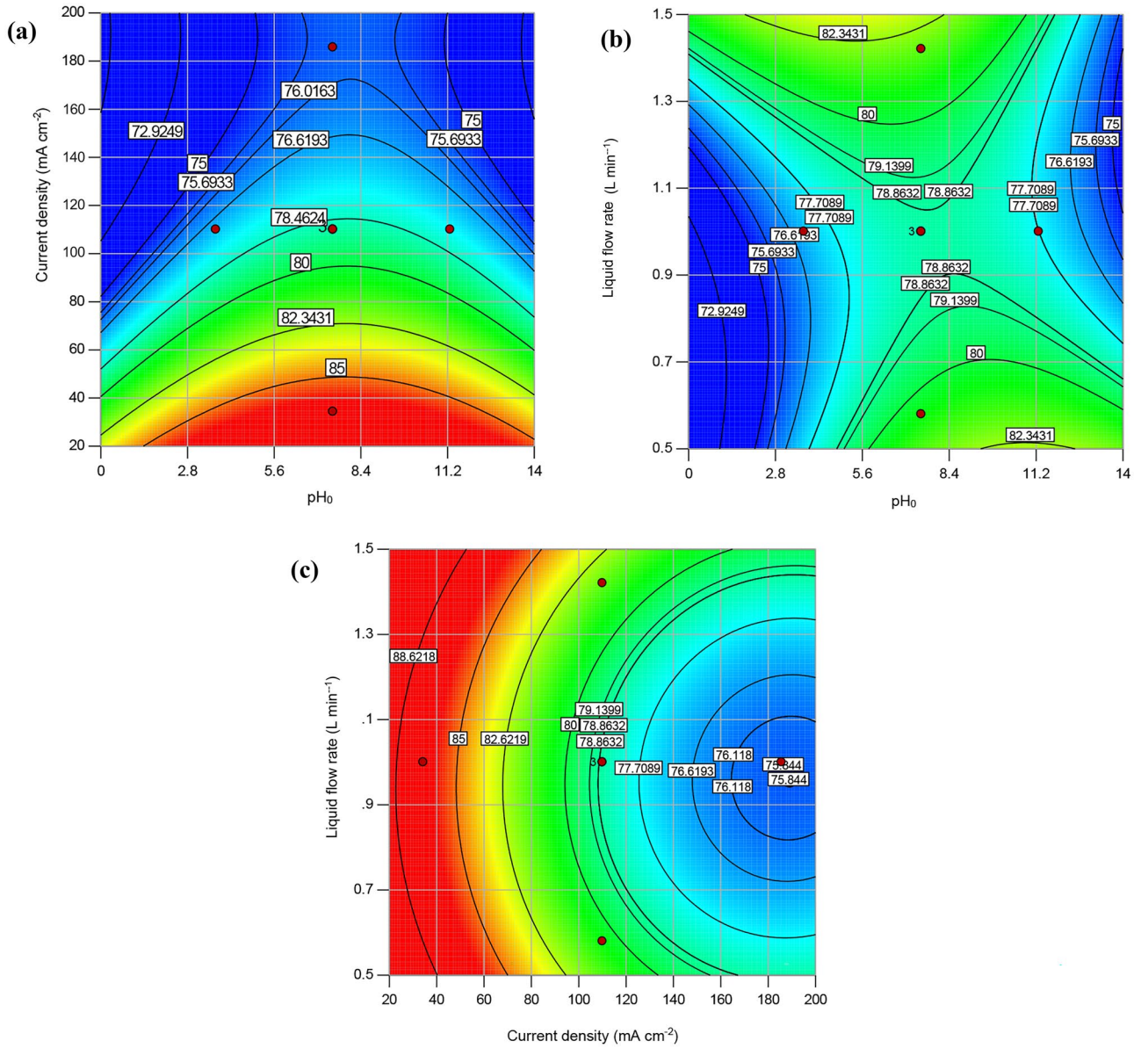

Fig. 4 Contour plot showing the effect of initial pH and current density (**a**), initial pH and liquid flow rate (**b**), and current density and liquid flow rate (**c**) on chloroquine degradation efficiency (η)

Even the objective function (η) not being strictly concave, the saddle point found can be called as a global maximum since it is the only one critical point of the objective function. Therefore, a local maximum can be called as a global maximum.

Model validation

To validate the set of optimal operating parameters found in the previous section, three complementary experiments were carried out under the optimal operating parameters found

Table 5 Solved convex optimization problem by using different numerical methods

η (%)	Method	Iteration	x_1	x_2 (mA cm^{-2})	x_3 (L min^{-1})	Characterization
89.30	IP	11	5.38	34.4	1.42	Local maximum
89.30	SQP	8	5.38	34.4	1.42	Local maximum
89.30	AS	7	5.38	34.4	1.42	Local maximum

SQP sequential quadratic programing, *AS* active-set, *IP* interior-point

Table 6 Optimal operating parameters of the electrochemical degradation of CQ

Optimal point	Value		Value		
pH_0	5.38	Response	Predicted	Experimental	Relative error (%)
j (mA cm^{-2})	34.40	η (%)	89.30	78.45 ± 0.43	12.14
Q (L min^{-1})	1.42				

by convex optimization, predicted, and observed values are listed in Table 6. The relative error (12.14%) reported in Table 6 indicates a good approximation of optimal operating conditions by the convex optimization method. Hence, the maximum electrochemical degradation efficiency of CQ was 89.3% at a pH_0 of 5.38, a j of 34.4 mA cm^{-2}, Q of 1.42 L min^{-1}, and 9 h of treatment time.

A *TOC* and *COD* analyses were performed according to the methodology described in the chemical analysis section. The initial and final values of *TOC* were 62.81 and 29.45 mg L^{-1}, respectively, while the initial and final values of *COD* were 82.67 and 40.0 mg L^{-1}, respectively. These values of *TOC* and *COD* achieve a mineralization efficiency and *COD* removal efficiency of 53.1 and 51.6%, respectively.

As has been known, the principal advantage of the advanced oxidation processes is the fact that a contaminant present in wastewater is transformed into carbon dioxide and ions. To evaluate the mineralization degree the mean oxidation number of carbon (*MOC*) has been computed by using Eq. (17) [51]. The *MOC* value must lie in the range of −4 to +4, and values outside this range indicate that *COD* or *TOC* was not determined correctly. Most compounds detected in aqueous solutions fall in the range of −2 to +3. In this case, the *MOC* varied from +1.44 to +1.96 indicating the presence of formic acid (*MOC* of +2) [52]. This compound is produced during the oxidation of organic molecules and its further oxidation leads to carbon dioxide. Hence, the electrochemical process employed herein is an adequate technology to carry out the electro-oxidation of CQ.

$$MOC = 4 - 1.5\frac{COD}{TOC} \tag{17}$$

Total operational cost

In order to compute the total operating cost, firstly the energy consumption was computed (0.041 kWh L^{-1} or 41 kWh m^{-3}) by using the Eq. (3) for U of 10.35 V, j of 34.4 mA cm^{-2}, A_e of 32 cm^2, t of 9 h, and V_s of 2.5 L. Consequently, the total operating cost (Cost) was computed by the set of Eqs. (3) to (4). Hence, the cost was 0.47 US$ L^{-1} when the FBER was operated at optimal operating conditions (pH_0 of 5.38, j of 34.4 mA cm^{-2}, Q of 1.42 L min^{-1} within 9 h of reaction time). This work is the only one that reports the associated cost (see Table 7).

Table 7 Electrochemical degradation of CQ under different wastewater treatment technologies

Process	Operating conditions	Electrodes		*Vs* (L)	Main results			
		Ca	An		ED (%)	EM (%)	Cost (US$ L^{-1})	Ref
E^O	[*CQ*] of 150 mg L^{-1} on 0.1 M de Na_2SO_4, pH_0 of 5.38, j of 134.4 mA cm^{-2}, Q of 1.42 L min^{-1} and 9 h	BDD	BDD	2.5	89.3	52.2	0.47	This work
PS^{NO}	[*CQ*] of 26 mg L^{-1}, pH of 7.4, O_2, UV of 320–600 nm and 3.5 h	—	—	0.1	100	—	—	[15]
AH^{NO}	[*CQ*] of 5.15 mg L^{-1}, pH of 6.8, 0.1 M of NaOH and 2 h	—	—	0.01	97.1	—	—	[54]
CO^{NO}	[*CQ*] of 50 mg L^{-1}, 20 mL H_2O_2 at 3% and 10 h	—	—	0.02	100	—	—	[55]
$EFEN^{NO}$	[*CQ*] of 125 mg L^{-1} on 0.05 M de Na_2SO_4, pH_0 of 3.0, j of 60 mA cm^{-2}, Q_{O2} of 80 mL min^{-1}, [Fe^{2+}] of 10 mg L^{-1}, Ω of 300 rpm and 5 h	G	BDD	0.5	100	92	—	[17]
P^{NO}	[*CQ*] of 5.04 mg L^{-1}, pH of 6.8, 30% O_2, UV-LC and 10 d	—	—	0.01	93.3	—	—	[54]

O optimized, *NO* not optimized, *Ca* cathode, *An* anode, V_s treated volume, *E* electrolysis, *PS* photochemical stabilization, *HA* alkaline hydrolysis, *CO* chemical oxidation with H_2O_2, *EFEN* electro-Fenton, *P* photochemical, *G* graphite, *BDD* Boron-doped diamond

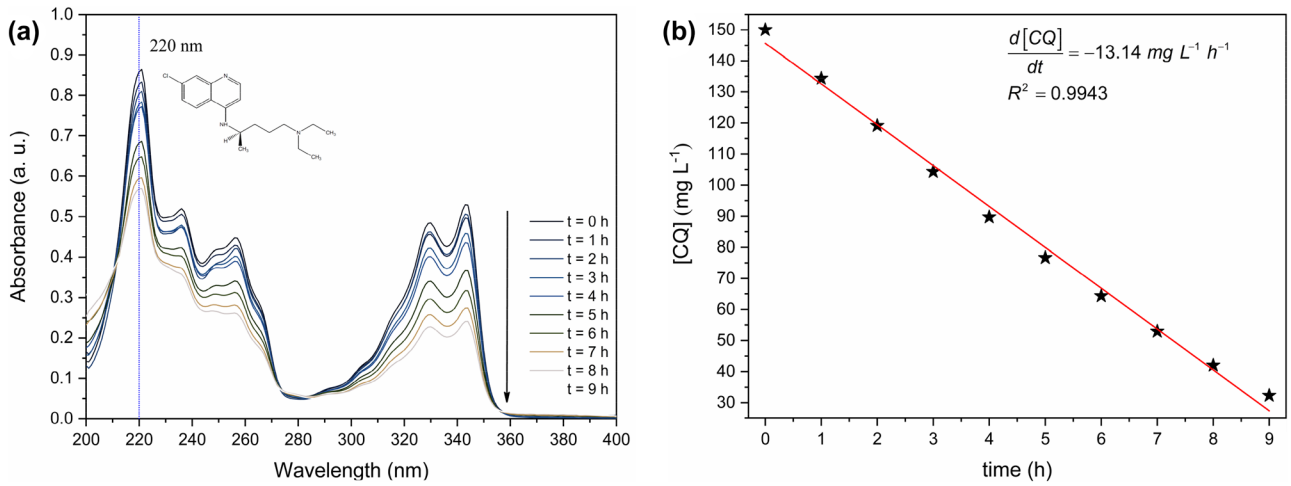

Fig. 5 **(a)** UV–Vis spectra for the CQ solution at different reaction times; **(b)** kinetic analysis for the pseudo-zero-order reaction of the CQ electrochemical degradation process

Kinetic modelling

Assuming that the electrochemical degradation of CQ proceeds mainly via hydroxyl radicals and neglecting the adsorption effect of CQ on the BDD electrode surface [53], a pseudo-zero-order kinetic model was tested to fit the experimental data (see Eq. (18)),

$$\frac{d[CQ]}{dt} = \underbrace{-k[^{\bullet}OH]}_{-k_{app}} = -k_{app} \tag{18}$$

A decrease in the absorbance maximum band of CQ (220 nm) was observed in Fig. 5a, as a function of reaction time. This behavior indicated that the degradation of CQ occurred by the breakup of the chemical structure of CQ by reaction with $^{\bullet}$OH produced during the electrooxidation reaction and, after that, forming other simple organic compounds. Also, this behavior suggests a constant production of $^{\bullet}$OH. To study the kinetics of the overall reaction involved in the CQ electro-oxidation, the decline of CQ concentration was considered. Figure 5b shows the kinetic behavior of the electrochemical degradation of CQ. The behavior displayed in Fig. 5b reveals a satisfactory pseudo-zero-order kinetic rate performance. From a linear regression analysis, the k_{app} value of 13.14 mg L^{-1} h^{-1} (2.54×10^{-5} mol dm^{-3} h^{-1}) was obtained with a determination coefficient (R^2) value of 0.9943. It is worth mentioning that the reported kinetic constant is a global oxidation constant since the oxidation of the intermediates by the produced hydroxyl radicals over time was not discriminated for its calculation. Nevertheless, being a pseudo-zero order process indicates that at the beginning of the treatment (when there was only CQ), the specific reaction rate is practically the same.

The found results in this research have been compared with previous reports (see Table 7). The electrochemical degradation efficiency of CQ in the literature is greater than that reported in this work. However, the volume of treated wastewater solution of CQ employed in literature (from 0.01 to 0.5 L) is lower than that used in the current research (2.5 L). Likewise, the initial concentration of CQ ($[CQ]_0 = 150$ mg L^{-1}) used in this work is greater than that employed in all references, which goes from 26 to 125 mg L^{-1}. Even though that 92% of *TOC* removal was achieved in reference [17], the volume treated (0.5 L) was 5 times lower than that employed in this work (2.5 L), and this may be the reason for the mineralization efficiency obtained in this work (52.2%) being lower than that in reference [17]. It should be noted that the current study is the only one that carries out the optimization of the degradation process of CQ and provides the associated cost (0.47 US$ L^{-1}). Based on the results found in this green wastewater treatment, it can be concluded that this green process is suitable for CQ removal.

Conclusions

Given the results of the current research paper, the ensuing conclusions are as follows:

- The degradation of chloroquine phosphate was successfully achieved in a flow-by electrochemical reactor employing two BDD electrodes and running in batch recirculation mode.
- The quadratic model to predict the degradation efficiency (η) in a flow-by electrochemical reactor equipped with two BDD electrodes was developed as a function of pH$_0$ (X_1),

j (X_2), and Q (X_3). Also, the most significant operational variable was found to be current density (j). This model is

$$\eta = 89.22 + 2.69X_1 - 0.17X_2 - 16.09X_3 + 0.0002X_1X_2 - 1.16X_1X_3 - 0.004X_2X_3 - 0.09X_1^2 + 0.0005X_2^2 + 13.29X_3^2$$

- The optimization of operational factors was satisfactorily attained by the convex optimization method. A global maximum (89.3%) was achieved at operational reaction conditions of $pH_0 = 5.38$, $j = 34.4$ mA cm^{-2}, and $Q = 1.42$ L min^{-1} within a treatment time of 9 h, employing an E_C of 0.041 kWh L^{-1} with a Cost of 0.47 US$ L^{-1}.
- Electrochemical degradation of CQ follows a pseudo-zero-order kinetic rate when the green process operates at optimal operation reaction conditions.
- The process evaluated in this investigation is a potential green process for wastewater treatment as it Babić S, Škorić I (2019) Thehas a low-cost (0.47 US$ L^{-1}), and no additional reagents must be added to perform the electrochemical degradation, and it is friendly with the environment.
- The oxidation number of organic carbon of the synthetic wastewater of CQ passed from + 1.44 to + 1.96 suggesting the presence of short-chain mono and dicarboxylic acids such as formic ($MOC = +2$).

Supplementary Information The online version contains supplementary material available at https://doi.org/10.1007/s10008-023-05452-7.

Acknowledgements The authors are grateful to Universidad del Mar for providing financial support of the research project CUP: 2II2104 (modeling and parametric optimization of the electrochemical mineralization of anti-COVID-19 drugs in a flow-by electrochemical reactor equipped with BDD electrodes). Also, the staff of the environmental and investigation laboratories is grateful for dedicating their time and effort to facilitate this research work.

Declarations

Competing interests The authors declare no competing interests.

References

1. OMS (2022) Weekly epidemiological update. In: World Health Organization. https://www.who.int/publications/m/item/weekly-epidemiological-update-on-covid-19---7-december-2022. Accessed 12 Dec 2022
2. Conacyt (2022) COVID-19 México. https://datos.covid-19.conacyt.mx/. Accessed 6 Dec 2022
3. Jin Y, Yang H, Ji W et al (2020) Virology, epidemiology, pathogenesis, and control of COVID-19. Viruses 12:372. https://doi.org/10.3390/v12040372
4. Plaze M, Attali D, Petit AC et al (2020) Repurposing of chlorpromazine in COVID-19 treatment: the reCoVery study. Encephale 46:S35–S39. https://doi.org/10.1016/j.encep.2020.04.010
5. Shrestha DB, Budhathoki P, Khadka S et al (2020) Favipiravir versus other antiviral or standard of care for COVID-19 treatment: a rapid systematic review and meta-analysis. Virol J 17:141. https://doi.org/10.1186/s12985-020-01412-z
6. Buckland MS, Galloway JB, Fhogartaigh CN et al (2020) Treatment of COVID-19 with remdesivir in the absence of humoral immunity: a case report. Nat Commun 11:6385. https://doi.org/10.1038/s41467-020-19761-2
7. Şimşek Yavuz S, Ünal S (2020) Antiviral treatment of covid-19. Turk J Med Sci 50
8. Calderón JM, Zerón HM, Padmanabhan S (2020) Treatment with hydroxychloroquine vs hydroxychloroquine + nitazoxanide in COVID-19 patients with risk factors for poor prognosis: a structured summary of a study protocol for a randomised controlled trial. Trials 21:504. https://doi.org/10.1186/s13063-020-04448-2
9. McCreary EK, Pogue Jason M on behalf of the S of IDP (2020) Coronavirus disease 2019 treatment: a review of early and emerging options. Open Forum Infect Dis 7:1–11. https://doi.org/10.1093/ofid/ofaa105
10. Pastick KA, Okafor EC, Wang F et al (2020) Review: hydroxychloroquine and chloroquine for treatment of SARS-CoV-2 (COVID-19). Open Forum Infect Dis 7:1–7. https://doi.org/10.1093/ofid/ofaa130
11. Kouznetsov VV, Amado Torres DF (2008) Antimaláricos: construcción de híbridos moleculares de la cloroquina. Univ Sci (Bogota) 13:306–320
12. Belayneh A (2020) Off-label use of chloroquine and hydroxychloroquine for COVID-19 treatment in Africa against WHO recommendation. Res Rep Trop Med 11:61–72. https://doi.org/10.2147/rrtm.s269936
13. Merino Argumánez C, Sáez de La Fuente I, Molina Collado Z et al (2017) La hidroxicloroquina, un fármaco potencialmente letal. Med Intensiva 41:257–259. https://doi.org/10.1016/j.medin.2016.05.004
14. Petrović M, Gonzalez S, Barceló D (2003) Analysis and removal of emerging contaminants in wastewater and drinking water. TrAC - Trends in Analytical Chemistry 22:685–696. https://doi.org/10.1016/S0165-9936(03)01105-1
15. Nord K, Karlsen J, Tønnesen HH (1991) Photochemical stability of biologically active compounds. IV. Photochemical degradation of chloroquine. Int J Pharm 72:11–18. https://doi.org/10.1016/0378-5173(91)90375-X
16. Coelho AS, Chagas CEP, de Pádua RM et al (2017) A comprehensive stability-indicating HPLC method for determination of chloroquine in active pharmaceutical ingredient and tablets: Identification of oxidation impurities. J Pharm Biomed Anal 145:248–254. https://doi.org/10.1016/j.jpba.2017.06.023
17. Midassi S, Bedoui A, Bensalah N (2020) Efficient degradation of chloroquine drug by electro-Fenton oxidation: effects of operating conditions and degradation mechanism. Chemosphere 260:127558. https://doi.org/10.1016/j.chemosphere.2020.127558
18. Dabić D, Babić S, Škorić I (2019) The role of photodegradation in the environmental fate of hydroxychloroquine - Science Direct. Chemospherere 230:268–277
19. Peralta E, Ruíz M, Martínez G et al (2018) Degradation of 4-chlorophenol in a batch electrochemical reactor using BDD electrodes. Int J Electrochem Sci 13:4625–4639. https://doi.org/10.20964/2018.05.21
20. Peralta-Reyes E, Natividad R, Castellanos M et al (2020) Electrooxidation of 2-chlorophenol with BDD electrodes in a continuous flow electrochemical reactor. J Flow Chem 10:437–447. https://doi.org/10.1007/s41981-020-00079-5
21. Regalado-Méndez A, Ruiz M, Hernández-Servín JA et al (2020) Electrochemical mineralization of ibuprofen on BDD electrodes in an electrochemical flow reactor: numerical optimization approach. Processes 8:1666. https://doi.org/10.3390/PR8121666

22. Maldonado S, Rodrigo M, Cañizares P et al (2020) On the degradation of 17-β estradiol using boron doped diamond electrodes. Processes 8:710. https://doi.org/10.3390/pr8060710
23. Barrera-Díaz CE, Frontana-Uribe BA, Rodríguez-Peña M et al (2018) Integrated advanced oxidation process, ozonation-electrodegradation treatments, for nonylphenol removal in batch and continuous reactor. Catal Today 305:108–116. https://doi.org/10.1016/j.cattod.2017.09.003
24. García-Orozco VM, Millán M, Lobato J et al (2020) Importance of electrode tailoring in the coupling of electrolysis with renewable energy. Chem Electro Chem 7:2925–2932. https://doi.org/10.1002/celc.202000550
25. Moreira FC, Boaventura RAR, Brillas E, Vilar VJP (2017) Electrochemical advanced oxidation processes: a review on their application to synthetic and real wastewaters. Appl Catal B 202:217–261
26. Frontana-Uribe BA, Little RD, Ibanez JG et al (2010) Organic electrosynthesis: a promising green methodology in organic chemistry. Green Chem 12:2099–2119. https://doi.org/10.1039/C0GC00382D
27. Huang KL, Chao PJ, Kuo YM et al (2021) Response surface methodology-based fabrication of boron-doped diamond electrodes for electrochemical degradation of guaifenesin in aqueous solutions. J Taiwan Inst Chem Eng 123:124–133. https://doi.org/10.1016/J.JTICE.2021.05.035
28. Wang L, Liang H, Huang H et al (2022) Performance analysis of a half-batch multi-cell three-dimensional electrode reactor for drilling wastewater: COD removal, energy consumption and hydrodynamic characteristic. Water Sci Technol 85:3343–3356. https://doi.org/10.2166/wst.2022.100
29. Bhagawati PB, Shivayogimath CB (2021) Electrochemical technique for paper mill effluent degradation using concentric aluminum tube electrodes (CATE). J Environ Health Sci Eng 19:553–564. https://doi.org/10.1007/s40201-021-00627-8
30. Matyasovszky N, Tian M, Chen A (2009) Kinetic study of the electrochemical oxidation of salicylic acid and salicylaldehyde using UV/vis spectroscopy and multivariate calibration. J Phys Chem A 113:9348–9353. https://doi.org/10.1021/jp904602j
31. Acosta-Angulo B, Diaz-Angulo J, Lara-Ramos J et al (2022) Analysis of the applications of particle swarm optimization and genetic algorithms on reaction kinetics: a prospective study for advanced oxidation processes. Chem Electro Chem 9:e202200229. https://doi.org/10.1002/celc.202200229
32. Viana DF, Salazar-Banda GR, Leite MS (2018) Electrochemical degradation of reactive black 5 with surface response and artificial neural networks optimization models. Sep Sci Technol 53:2647–2661. https://doi.org/10.1080/01496395.2018.1463264
33. Demir A, Geçgel C, Gören N (2022) Electrochemical degradation of favipiravir (anti-viral) drug from aqueous solution: optimization of operating parameters using the response surface method. Environ Technol 1–18. https://doi.org/10.1080/09593330.2022.2091483
34. Ramírez C, Saldaña A, Hernández B et al (2013) Electrochemical oxidation of methyl orange azo dye at pilot flow plant using BDD technology. J Ind Eng Chem 19:571–579. https://doi.org/10.1016/J.JIEC.2012.09.010
35. Moteshaker PM, Rokni SE, Farnoodian N et al (2020) Application of response surface methodology for optimization of electrochemical process in metronidazole (MNZ) removal from aqueous solutions using stainless steel 316 (SS316) and lead (Pb) anodes. Int J Chem Reactor Eng 18:1–14. https://doi.org/10.1515/ijcre-2020-0055
36. Wang H, Lei He, Xiaoya Chen et al (2021) Influence of process parameters on electrochemical removal of indole: response surface methodology, mechanism and energy consumption. Int J Electrochem Sci 16:21039. https://doi.org/10.20964/2021.03.54
37. Sigma-Aldrich (2022) Safety data sheet of chloroquine phosphate. In: Sigma-Aldrich. https://www.sigmaaldrich.com/MX/es/sds/sigma/c6628. Accessed 28 Jan 2023
38. ChemSpider (2023) Chloroquine. In: Royal Society of Chemistry. http://www.chemspider.com/Chemical-Structure.2618.html. Accessed 28 Jan 2023
39. Tariq M, Al-Badr AA (1984) Chloroquine. In: Florey K (ed) Analytical Profiles of Drug Substances. Academic Press, pp 95–125
40. Guoquan Z, Tinggong W, Danfeng S et al (2021) The solubility and dissolution thermodynamic properties of chloroquine diphosphate in different organic solvents. J Chem Thermodyn 156:106368. https://doi.org/10.1016/J.JCT.2020.106368
41. Regalado-Méndez A, Mentado-Morales J, Vázquez CE et al (2018) Modeling and hydraulic characterization of a filter-press-type electrochemical reactor by using residence time distribution analysis and hydraulic indices. Int J Chem Reactor Eng 16:20170210. https://doi.org/10.1515/ijcre-2017-0210
42. Baird RW, Eaton AD, Rice EW (2017) Standard methods for the examination of water and wastewater, 23rd edn. American Public Health Association, Washington, DC
43. Aziz SQ, Aziz HA, Yusoff MS, Bashir MJK (2011) Landfill leachate treatment using powdered activated carbon augmented sequencing batch reactor (SBR) process: optimization by response surface methodology. J Hazard Mater 189:404–413. https://doi.org/10.1016/j.jhazmat.2011.02.052
44. Regalado-Méndez A, Báez-González JG, Peralta-Reyes E, Trujillo-Tapia MN (2010) Problem based learning: Obtaining enzyme kinetics parameters integrating linear algebra, computer programming and biochemistry curriculum. In: Technological Developments in Networking, Education and Automation
45. Muhamad MH, Sheikh Abdullah SR, Mohamad AB et al (2013) Application of response surface methodology (RSM) for optimisation of COD, NH_3–N and 2,4-DCP removal from recycled paper wastewater in a pilot-scale granular activated carbon sequencing batch biofilm reactor (GAC-SBBR). J Environ Manage 121:179–190. https://doi.org/10.1016/j.jenvman.2013.02.016
46. Montgomery DC (1984) Design and analysis of experiments, Second edi. Wiley, New York
47. Michaud P-A, Panizza M, Ouattara L et al (2003) Electrochemical oxidation of water on synthetic boron-doped diamond thin film anodes. J Appl Electrochem 33:151–154. https://doi.org/10.1023/A:1024084924058
48. Brillas E, Sirés I, Arias C et al (2005) Mineralization of paracetamol in aqueous medium by anodic oxidation with a boron-doped diamond electrode. Chemosphere 58:399–406. https://doi.org/10.1016/J.CHEMOSPHERE.2004.09.028
49. Thomas FE, Himmelblau DM, Lasdon LS (2001) Optimization of chemical processes, 2nd edn. McGraw-Hill, New York
50. Sinha SM (2006) Convex and concave functions. In: Mathematical Programming. Elsevier, pp 94–114
51. Vogel F, Harf J, Hug A, von Rohr PR (2000) The mean oxidation number of carbon (MOC)—a useful concept for describing oxidation processes. Water Res 34:2689–2702. https://doi.org/10.1016/S0043-1354(00)00029-4
52. Donoso G, Dominguez JR, González T et al (2021) Electrochemical and sonochemical advanced oxidation processes applied to tartrazine removal. Influence of operational conditions and aqueous matrix. Environ Res 202:111517. https://doi.org/10.1016/J.ENVRES.2021.111517
53. Martí-Calatayud MC, Dionís E, Mestre S, Pérez-Herranz V (2022) Antimony-doped tin dioxide ceramics used as standalone membrane electrodes in electrofiltration reactors enhance the oxidation of organic micropollutants. J Clean Prod 363:132342. https://doi.org/10.1016/j.jclepro.2022.132342
54. Rivas-Granizo P, Jorge Santos SRC, Ferraz HG (2009) Development of a stability-indicating LC assay method for determination of chloroquine. Chromatographia 69:137–141. https://doi.org/10.1365/s10337-009-0985-3

55. Doddaga S, Peddakonda R (2013) Chloroquine-N-oxide, a major oxidative degradation product of chloroquine: Identification, synthesis and characterization. J Pharm Biomed Anal 81–82:118–125. https://doi.org/10.1016/J.JPBA.2013.04.004

Publisher's Note Springer Nature remains neutral with regard to jurisdictional claims in published maps and institutional affiliations.

Springer Nature or its licensor (e.g. a society or other partner) holds exclusive rights to this article under a publishing agreement with the author(s) or other rightsholder(s); author self-archiving of the accepted manuscript version of this article is solely governed by the terms of such publishing agreement and applicable law.